

# A SIMPLE MODEL FOR THE EVOLUTION OF EVOLUTION

Siegfried Fussy, Gerhard Grössing and Herbert Schwabl

*Austrian Institute for Nonlinear Studies,  
Parkgasse 9, A-1030 Vienna, Austria*

## Abstract

A simple model of macroevolution is proposed exhibiting both the property of punctuated equilibrium and the dynamics of potentialities for different species to evolve towards increasingly higher complexity. It is based on the phenomenon of fractal evolution which has been shown to constitute a fundamental property of nonlinear discretized systems with one memory- or random-based feedback loop. The latter involves a basic “cognitive” function of each species given by the power of distinction of states within some predefined resolution. The introduction of a realistic background noise limiting the range of the feedback operation yields a pattern signature in fitness space with a distribution of temporal boost/mutation distances according to a randomized devil’s staircase function.

Introducing a further level in the hierarchy of the system’s rules, the possibility of an adaptive evolutionary change of the resolution itself is implemented, thereby providing a time-dependent measure of the species’ cognitive abilities: an additional feedback loop makes use of the inevitable intrinsic fluctuations within the fitness landscape to direct the temporal change of the resolution. Feeding back the small adaptive changes of resolution into the essentially directionless variations of the patterns’ lifetimes in fitness space effectively leads to a clear tendency towards increasing evolution potentials for each species (“hierarchically emergent fractal evolution”).

*Keywords:* Macroeolution, punctuated equilibrium, fractal evolution, growth of complexity

# 1 Introduction: Punctuated equilibrium and self-organized criticality

Punctuated equilibrium is a well-documented extension of Darwinian evolutionary theory [7, 13]. On a population level, it has recently been observed in the laboratory: during its evolution, the average cell size of *Escherichia coli* bacteria showed long periods of stasis with rare beneficial mutations rapidly sweeping through the whole population [8, 15]. Presently, however, it is not yet clear, whether punctuations in the domain of populations and species, respectively, are unrelated, or consequences of the same evolutionary mechanisms at work. On the species level, some of the qualitative features of punctuated equilibrium have been successfully simulated by Bak and Sneppen [3] in a toy model on a lattice of sites, with each site representing a species, thereby drawing on earlier work on self-organized criticality (SOC) [4]. Recently, exact results have been obtained for spatiotemporal evolutions in an extended SOC model of punctuated equilibrium with many internal degrees of freedom per site [6], for a model with neural-like rules [19], and for generating phylogenetic-like trees [20]. However, the successful implementation of SOC models notwithstanding, there exists one important question which is hardly touched upon by these models, namely how evolution produces entities of increased complexity. In particular, it has been proposed by Kauffman and coworkers that the Darwinian process of mutation and environmental selection would have to be complemented by self-organizing processes in order to eventually decouple the strict link between mutation and selection [14].

In this paper we present a simple toy-model of evolution which is general enough to be compatible with SOC models of punctuated equilibrium, but in essential ways goes beyond them to encompass evolution towards higher complexity. For, if one considers the Bak-Sneppen model and its more recent versions, one is led to conclude that the SOC state is always a “quasi - steady state”, i.e., “the evolution process always self-organizes into the same critical steady state having, as a consequence, the same appearance” [1]. In other words, the analogy to the well-known sandpile model suggests that SOC describes evolution via punctuated avalanches of high mutation rates over a wide range of sizes, with long intermittent periods of stability, but without any (long term) time dependence of the avalanche sizes, the equilibrium periods, or their relative changes, respectively. This overall large-scale time symmetry is inherent in the model of Bak and Sneppen, as is easily seen from its results.

In their one-dimensional case that interests us here, each site on a lattice representing a species interacts with its two nearest neighbors (thus representing a food chain, for example). The individual species (sites) are assigned random numbers between 0 and 1 representing their fitness in the fitness landscape of the whole evolving pattern of lattice sites. At each time step, the site with the lowest fitness is chosen to be replaced by a different random number, thus mimicking Darwinian extinction of the least fit species and its replacement with another species in the same ecological niche. The same procedure is also applied to the

two nearest neighbors of the least fit species to simulate coevolution, so that in sum the fitness values of three sites are changed per time step. The result of this procedure is that most species self-organize into uniform distribution above some critical fitness value, while the few below it produce said punctuated avalanches of various sizes. The resulting activity pattern for the mutations clearly shows punctuated equilibrium behavior which is time-symmetric over long periods of evolutionary time (cf. Fig. 6 in [2]). Moreover, as the model allows to add together only accumulated mutations at single sites, i.e., without differentiating between progress and regression in fitness over time, the accumulated activity pattern is also time-invariant (cf. Fig. 7 in [2]), and has recently been identified with the fractal pattern of a randomized devil's staircase function [6].

In contrast, we design our toy model in such a way that four major problems are directly addressed to overcome some weak points in the existing models of punctuated equilibrium:

1) To potentially allow for the emergence of ever higher complexity, the implicit overall time-symmetry of the evolving patterns in state-space must be discarded.

2) Accordingly, a plot of evolutionary changes for a single species over time must not only add accumulated changes (producing a devil's staircase function), but must be able to differentiate between progress and regression with regard to some measure of fitness or complexity (cf. Fig. 1 in [8] and Fig. 1A in [18]).

3) The strict coupling between mutation and selection, i.e. the ongoing and strictly time-ordered interplay of both mechanisms, which is often considered as a necessary prerequisite for evolution, has to be relaxed to allow for the self-organization of evolutionary patterns. In this way, coevolutionary processes can lead to an effective decoupling of mutation and selection.

4) As the model to be designed should depend even less on the concrete content of micro-evolution, it should be as abstract as possible to study potential trends in evolution with a high chance for universality, i.e., irrespective of the underlying detailed processes. We thus aim at a meta-macroevolutionary model in the sense that we disregard questions on the concrete evolutionary substrate, thereby concentrating on relative changes with respect to previous evolutions. In other words, we are interested in simulating the "evolution of evolution". Also, as far as the assumption holds that the same evolutionary mechanisms are at work at the levels of populations and species, respectively, our model for the species level will apply to the population level as well.

To implement the four points just mentioned, we propose the following simple toy-model for the evolution of evolution.

## 2 Hierarchically emergent fractal evolution (HEFE) with noise

### 2.1 Fractal evolution

We consider the evolution in time of a one-dimensional array of cells  $\rho_0(t, j)$  with  $j = 1, \dots, N$  representing the number of species on a coupled map lattice (CML). The nearest neighbor interaction implemented is of the form

$$\rho_0(t, j) = \frac{1}{\mathcal{N}_0(t)} \{ \rho_0(t-1, j) + \delta \cdot [\rho_0(t-1, j-1) + \rho_0(t-1, j+1)] \} \quad (1)$$

$$j = 1, \dots, N, \quad \rho_0, \delta \in \mathcal{R}$$

with  $\delta$  as coupling constant and  $\mathcal{N}_0$  as normalization factor yielding

$$\sum_{j=1}^N \rho_0(t, j) = 1 \quad \text{for all } t. \quad (2)$$

To constrain the values of the sites within a realistic domain, we introduce a system's *internal* precision limit  $\xi_{max} = 10^{-6}$  with the effect that each site  $\rho_0(t, j) \leq \xi_{max}$  is replaced by a white noise term, generated by  $\xi_{max} \cdot RAN$ . The random number  $RAN$  is uniformly distributed on the interval  $[0, 1]$ .

In this way,  $\rho_0(t)$  assumes values between zero and one representing the individual species' fitness at time step  $t$  relative to the others in such a manner that the total fitness for the whole array is given by a constant which, without loss of generality, is defined to be equal to unity. In other words, just as in [3], we assume local interaction between the nearest neighbored species to affect relative fitness. However, as opposed to [3], we are not interested in implementing a very specific and thus extremely model-dependent mechanism of eliminating least fit species, or the like. Rather, we intend to study the *relative frequency of deviations from some average evolution*, the details of which are not supposed to matter. To do so, we need to have an evolution of the form of Eq. (1) upon which certain constraints can be imposed, such that some kind of statistically controllable but individually contingent deviation can be implemented.

With regard to this, a phenomenon is at hand which has been discovered and studied by us in some detail, called *fractal evolution* [9, 10]. It is a universal dynamic property shown for one-dimensional CMLs with (i) one or more temporal feedback operations (involving some memory of the system's states) boosting certain sites to values far above the average ones, and (ii) a normalization procedure after each time step as given by Eq. (2). Fractal evolution is characterized by a power-law behavior of the system's order parameter with regard to a resolution-like parameter which controls the deviation from an undisturbed (i.e., feedback-less) system's evolution and provides a dynamically invariant measure for the emerging spatiotemporal patterns [9]. It must be strictly distinguished from the phenomenon of fractal growth, which describes the accumulation of micro-patterns into a static structure with (self-similar or other scale invariant) fractal features. In contrast, fractal evolution is characterized by the fact that

the dynamics of the evolution itself is scale invariant: instead of generating a “frozen” fractal object, the generation mechanism itself is “fractal”, i.e. the chosen resolution itself finally generates the observed fractal properties. In reference [10] we showed that the phenomenon is very robust with respect to variation of the system’s variables and holds also if, instead of a temporal feedback condition, the deviations from the average evolution are implemented by randomly generating local boosts to high values for individual sites. In these cases, the only difference to the feedback situation is a different resulting fractal evolution exponent in the power law. This means that no matter how the detailed micro-evolutionary substrate is implemented, i.e. by either entirely deterministic temporal feedback loops with a memory, or by completely random boosts to produce patterns deviating from the average development of the system, fractal evolution will be observed in most cases [10].

In the following, we shall choose temporal feedback loops in our model because they introduce a quality of self-reference for the whole system which can be expanded upon later (cf. Sec. 2.2). As a concrete motivation for doing so, we consider a certain periodicity of constraining conditions for the whole evolutionary landscape. Again, the details are not supposed to matter, i.e., the periodicity may refer to relatively short-term cycles of constraints enforcing functional couplings within individual species, or externally, in the ecology or the like. However, the period of constraints should also not be too short, because otherwise internal fluctuations would merely produce spurious effects of the internal systems dynamics which are of no particular interest here.

In a “normal” evolution of our landscape that were unaffected by such cycles, the relative fitness values would gradually become adjusted to each other, thus gradually reaching an ever more smeared-out pattern representing stasis or equilibrium. However, if a species’ fitness value after such a cycle happens to be the same again as before it, within a certain degree of accuracy  $1/\epsilon$ , then, even if the relative fitness value is low, some reproductive isolation must have been achieved (for example, via economic functional couplings) that amounts to an acquisition of a relative survival rate far above the average. In fact, “molecular cognition” within genomic dynamics [17] already suggests a certain cognitive ability for each individual site in that it can monitor its own “fitness” within that of its environment with a resolution  $1/\epsilon$ . Maintaining constancy in fitness space within cycle periods with a constraining and eventually destructive potential, while most of the environment produces decreasing fitness values, means that an ecological niche has been found whose fitness potential can be consumed. (The overall relative fitness is thus decoupled from the individual and momentary survival rate: the former is a purely coevolutionary measure, while the latter refers to a concrete situation in the larger context of cyclically changing constraining conditions of the whole evolutionary landscape.) In these cases, then, the species’ site is a particularly favorable niche and therefore enhanced to some boost value, thus providing a fragmented overall pattern emerging in fitness space with particular elevated zones of highest survival rates (and, consequently, also of fitness).

These zones represent a high possibility for reproductive isolation (for ex-

ample on the population level) and thus also for protected change. Although in principle it can occur at any time or site, a species' possible mutation, then, is most likely to accumulate into an evolutionarily conserved change (for example a morphological one) if occurring in such boosted niches of survival rates (and thus also new fitness values) far above the average. Naturally, if the accuracy  $1/\epsilon$  within which present and past relative fitness values are observed (i.e., to produce constancy with respect to the steadily evolving environment) is rather low, there will be a relatively high chance for various boosts to occur within short periods of time. If, on the other hand,  $1/\epsilon$  becomes higher and higher, i.e., if the cognitive requirements regarding the resolution become ever more demanding, then the chance for boosts gradually diminishes, and the actually boosted patterns will survive for longer periods of time.

To implement said temporal feedback operation in our model of Eq. (1), we install an enhancement (of strength  $A_{amp}$ ) of each site  $\rho(t, j) > \xi_{max}$  fulfilling an  $\epsilon$ -condition

$$\begin{aligned} \rho(t, j) &= \frac{1}{N(t)} \{ [A_{amp} - \rho_{0,\xi}(t, j)] \cdot \theta_\epsilon \cdot \theta_{mem} \cdot \theta_\xi + \rho_{0,\xi}(t, j) \} \\ &\quad \text{with} \\ \rho_{0,\xi}(t, j) &= [\rho_0(t, j) - \xi] \cdot \theta_\xi + \xi, \quad \rho_0(t, j) \text{ defined in Eq. (1)}, \\ \xi &= \xi_{max} \cdot RAN, \quad RAN \in [0, 1], \quad \theta_\xi = \Theta(\rho_0(t, j) - \xi_{max}), \\ \theta_\epsilon &= \Theta \left( \epsilon - \left| \frac{\rho_{0,\xi}(t, j)}{\rho(t - t_{mem}, j)} - 1 \right| \right), \quad 0 \leq \epsilon \leq 1 (= 100\%), \quad \theta_{mem} = \Theta(t - t_{mem}), \\ &\quad \text{and} \quad \Theta(x) = \begin{cases} 1 & : x > 0 \\ 0 & : x \leq 0 \end{cases}. \end{aligned} \tag{3}$$

As usual, we impose periodic boundary conditions. Also, we introduce a time span  $t_{mem}$  during which the system's memory is effective. (For example, the latter may reflect the maintainance of a particular molecular state during one cycle of the periodical constraining conditions.)

In other words, the enhancement for any site  $\rho_{0,\xi}(t, j) > \xi_{max}$  takes place if  $t > t_{mem}$  (i.e., the time span during which a system's memory is effective) and if the condition  $\rho(t - t_{mem}, j) \cdot (1 - \epsilon) < \rho_{0,\xi}(t, j) < \rho(t - t_{mem}, j) \cdot (1 + \epsilon)$  is fulfilled. Note that this kind of feedback operation simulates a selection process enhancing the values and, consequently, the further evolutions of those sites which are comparable in fitness with their corresponding values in the past since they fulfill the  $\epsilon$ -condition.

The whole normalized system is constrained to the range  $0 \leq \rho(t, j) \leq 1$ . Values of  $\rho(t, j) \leq \xi_{max}$  are, just for simplicity, replaced by white noise terms, i.e., in that case, whatever kind of noise existing in our system exceeds a signal generated by the system's rules. Moreover, a further parameter is introduced as an *external* representation threshold  $L \gg \xi_{max}$ : with it a background is defined against which the arising patterns obeying  $\rho(t, j) \geq L$  can easily be discerned. Otherwise, e.g. for  $L = \xi_{max}$ , the evolving systems' pattern would appear as one connected stream and could not be discerned into the separated fragments of the landscape's peaks needed for quantitative analysis.

For the further analysis and without loss of generality (cf. the discussion

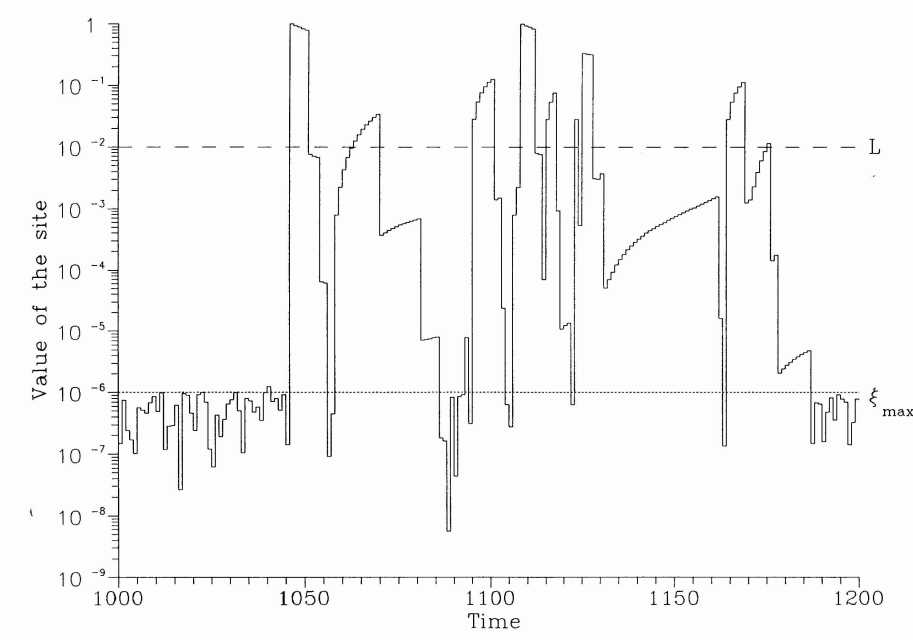


Figure 1: Temporal evolution of an arbitrary site (#48), initiating from the noise domain below the threshold  $\xi_{max}$ , and later entering the region of an observable pattern above the representation threshold  $L$ .

below) we choose a default set of parameter values:

$$\begin{aligned}
 \text{Number of sites (dimension)} \quad & N = 120 \\
 \text{Initial values (before normalization)} \quad & \rho(0, 40) = 0.1, \rho(0, 60) = 0.9, \rho(0, 100) = 0.3 \\
 \text{Mixing parameter (coupling constant)} \quad & \delta = 0.03 \\
 \text{Boost value (enhancement)} \quad & A_{amp} = 100 \\
 \text{Size of memory} \quad & t_{mem} = 200 \\
 \text{Threshold value} \quad & L = 10^{-2}
 \end{aligned} \tag{4}$$

In Figure 1 the time evolution due to Eq. (3) of one arbitrarily chosen site (i.e., site #48 in our case) is displayed together with the noise threshold (dotted line) and the external representation threshold used in the further graphical representation of the plots (dashed line). Due to Eq. (3), at time steps  $t = 1046$  and  $t = 1108$  the site is boosted up to a value of order  $O(1)$  after normalization, whereupon the typical decrease due to the diffusion rule (1) is observed until the boost of some other site within the array suppresses it by the factor  $A_{amp} = 100$  due to the normalization procedure. The feature of repeated staircase-like increases of the site's values comes from contributions of neighbored large-valued sites.

A spatiotemporal plot of all sites above the threshold value  $L$  is shown in

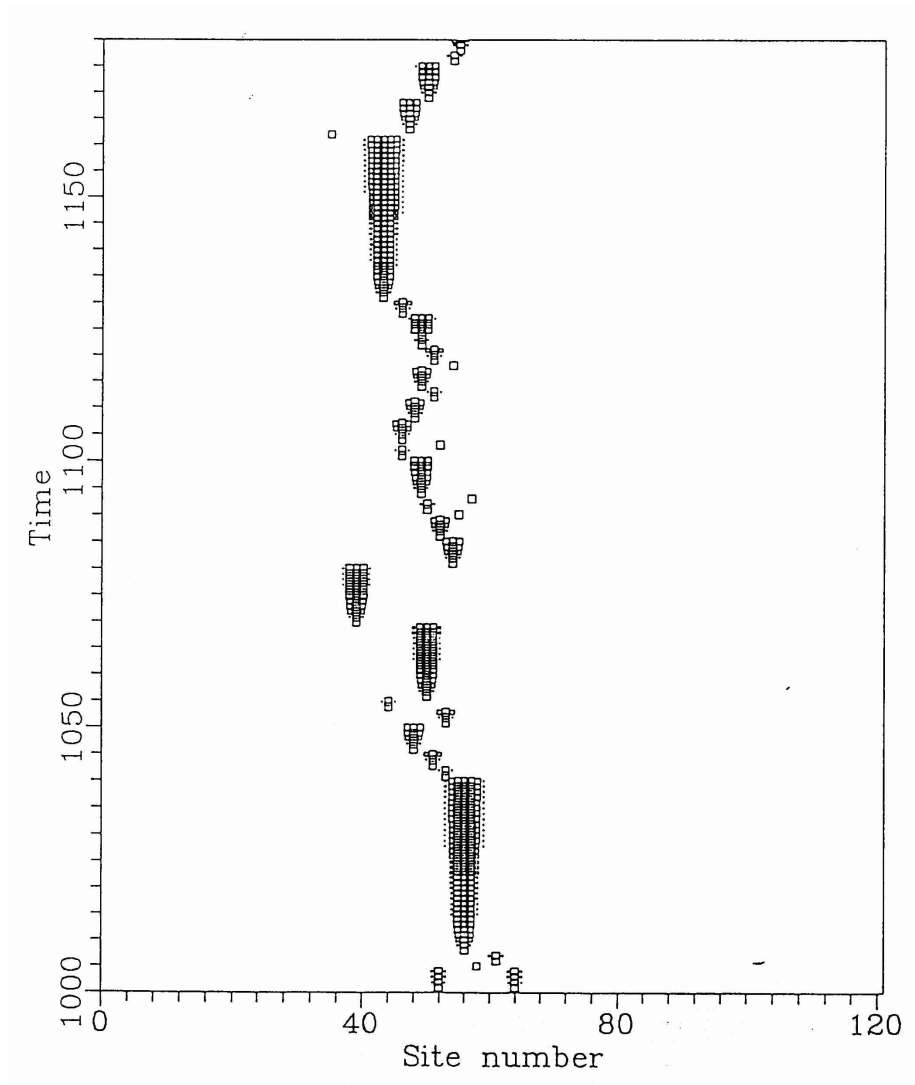


Figure 2: Density plot of the evolving system accentuating the range of the box values from  $L = 10^{-2}$  to  $10^{-1}$ . Values larger than  $10^{-1}$  are displayed with the maximal box size. The relative interval width  $\epsilon$  is chosen as  $\epsilon = 30\%$ .



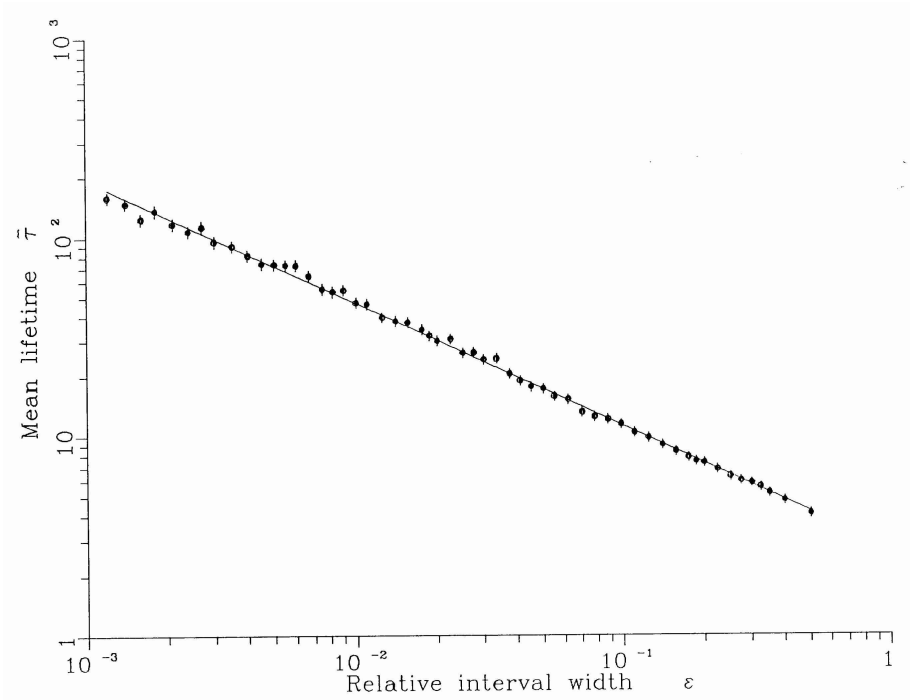


Figure 3: Log-log plot of the mean lifetimes  $\tilde{\tau}$  of the fragments versus the relative interval width  $\epsilon$ . System parameters are taken from Eq. (4). The fractal evolution exponent is estimated by the slope of the fit curve.

Figure 2. Contrary to the signature of fractal evolution introduced in [9, 10], the fragments gather around a narrow array and are not distributed over the whole spatiotemporal plane. This effect represents a certain “taming” of evolutionary chance and comes from the restriction requiring that all sites be larger than the noise threshold  $\xi_{max}$  for their possible enhancement. (As stated above, eventual values below the noise threshold thus contribute only to the noise itself, but cannot be boosted to values dominating the whole evolution.) Since the range of those values which are checked by the  $\epsilon$ -condition of (3) contains only six orders of magnitude, a boosted site will be placed in the spatial neighborhood of a fragment  $t_{mem}$  time steps ago. As will be shown below, this “stream-like” feature in the fitness landscape is crucial for the punctuated equilibrium behavior during the systems evolution.

In Figure 3 the system’s global property of fractal evolution is shown. The mean lifetime  $\tilde{\tau}$  of the patterns which is estimated by the arithmetic mean of the maximal temporal extension of all fragments for a chosen  $\epsilon$  (cf. Figure 2) scales according to

$$\tilde{\tau} = a \cdot \epsilon^b, \quad \text{with } a = 2.69 \pm 0.05, \quad b = -0.620 \pm 0.005, \quad (5)$$

practically irrespective of variations of the systems variables or the initial conditions. The power-law behavior of the system's order parameter  $\tilde{\tau}$  with regard to the resolution-like parameter  $\epsilon$  provides a dynamically invariant measure for the emerging spatiotemporal patterns given by the fractal evolution exponent  $b$ . As will be discussed in Sec. 2.2, fractal evolution in its dynamic sense is obtained only if the restriction to one specific value of  $\epsilon$  is abolished. Note that the system evolving under a chosen  $\epsilon$  does not evolve automatically towards a critical state in the sense of the SOC theory [4] since the avalanches of the fragments' sizes do not occur in our system on all scales.

Although the two concurring conditions in Eq. (3), i.e. the temporal  $\epsilon$ -condition and the noise-threshold condition, constrain the evolving patterns to lie within a narrow range, the long-term behavior as shown in Figure 4 exhibits a random-walk-like movement of the stream of fragments across the whole array. The invariance of this ergodic-like property under variation of the systems parameters has been checked empirically. Even the replacement of white noise values for sites below  $\xi_{max}$  by a constant value (by  $10^{-7}$ , for example), provides the observed ergodicity, although the stream of fragments then evolves symmetrically due to the totally symmetric evolution rule and the uniform background. Therefore, in the long run, practically each site/species gets the chance to obtain a high survival rate and, consequently, to evolve in a high fitness potential.

Any enhancement of a site represents a strong intervention for the system as a whole (due to the normalization) and for the represented species itself, of course, since it can be interpreted both as a drastic change in coevolutionary fitness or as a site-bound beneficial mutation, respectively. Consequently, the time span between two succeeding boosts for any site offers both the opportunity for further beneficial selection during its evolution, or towards ever decreasing fitness, and ultimately being swept below the noise limit ("detrimental extinction"). In Figure 5 the accumulated boosts are displayed for a time interval of 50000 time steps. Similar to the SOC models [2, 6], each site exhibits a punctuated equilibrium behavior with respect to the time plateaus indicating the time difference between two drastic evolutionary activities. Due to the chosen initial conditions and within the first 50000 time steps, site #30 happens to experience many more changes than site #10.

Since the stream of fragments and thus the main boost activities will reach also previously quiescent regions after some time (cf. Figure 4), the accumulated boosts of site #10 will eventually catch up with those of site #30. The dashed curve in Figure 5 shows the effect of omitting only one boost (i.e., the 100th one in our case) during the site's evolution. The observed dramatic change of the accumulation curve demonstrates just one example of the crucial role of contingency in the systems dynamics.

The analysis of the distributions of time plateaus for an arbitrarily chosen site yields a (discretized) shape as shown in Figure 6. Each bin contains the relative frequency of ten succeeding plateau sizes. Apparently, practically all sizes of periods of stasis are present, the data for bin #2 up to about #20 even lying on a straight line in a log-log plot. The peaks around bin #20, i.e. for plateau sizes of order  $O(200)$ , and another, weaker one around bin #40 (plateau

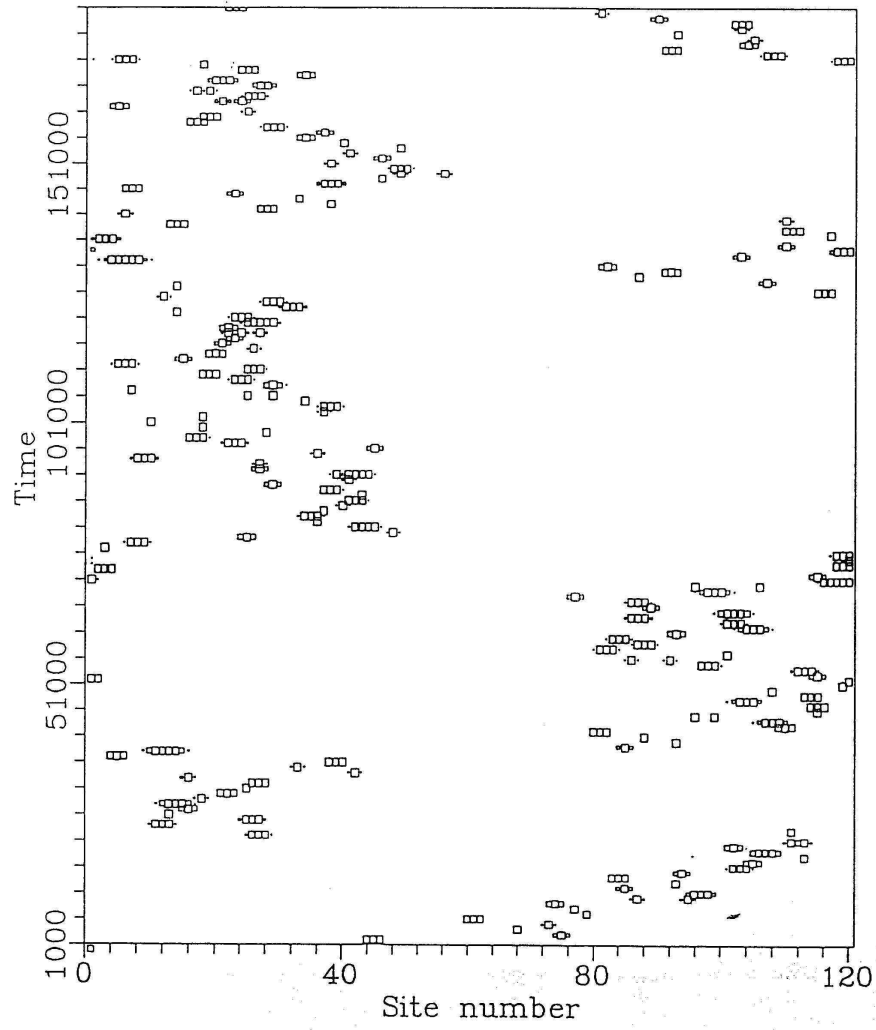


Figure 4: Same as in Figure 2, but now only for each 1000th time step, in order to see the long-term evolution. The narrow band of fragments in Figure 2 eventually enters practically all regions of the array in a random-walk-like manner.

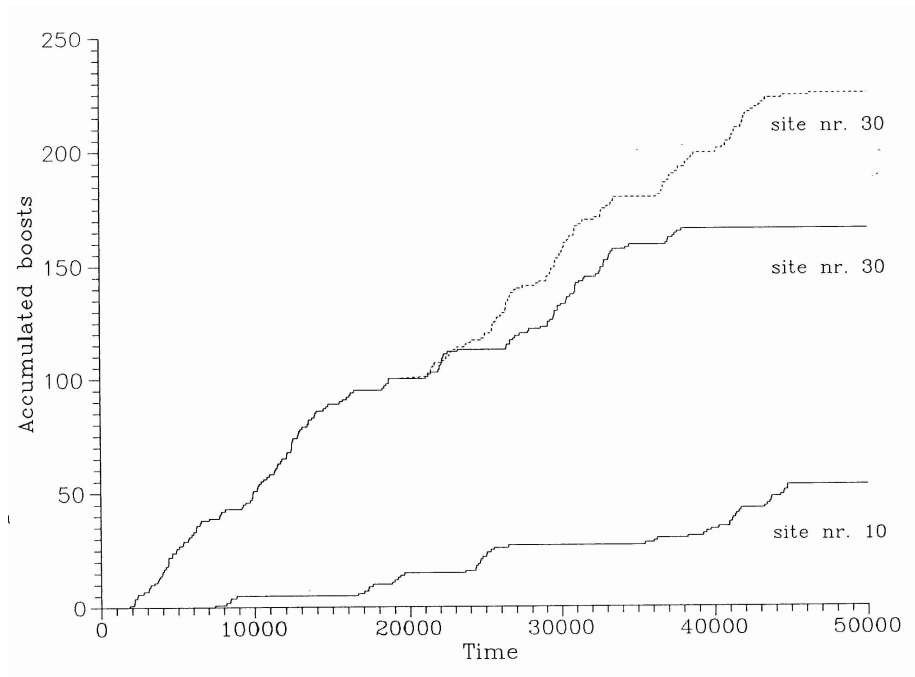


Figure 5: The accumulated boosts for two different sites show punctuated equilibrium behavior, i.e., periods of stasis are interrupted by high activity of boosts including eventual mutations. The dashed line shows the effect of omitting the 100th boost for site #30.

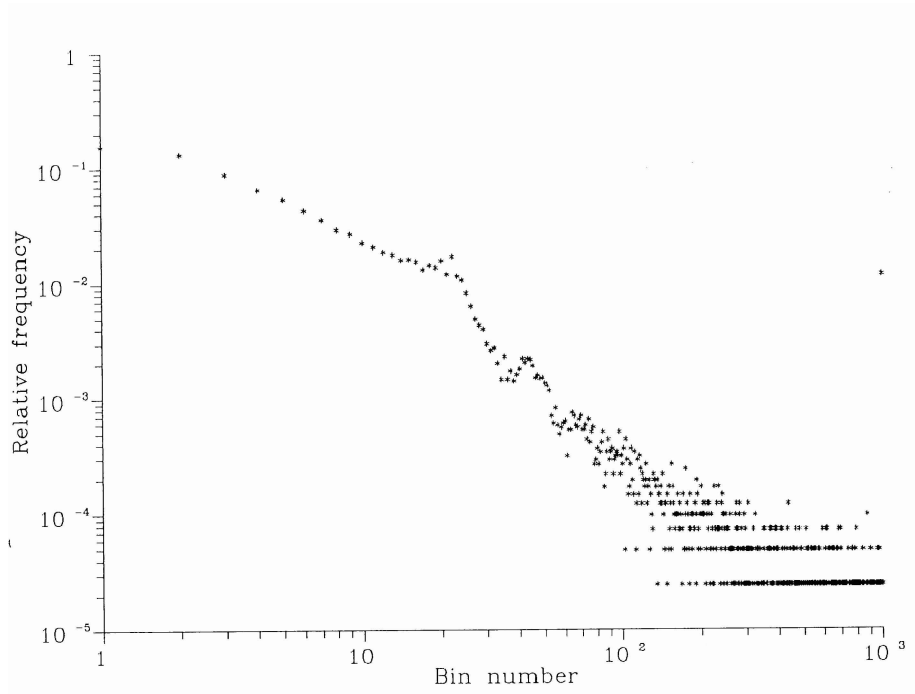


Figure 6: Relative frequency distribution of the sizes of the time plateaus in Figure 5 according to their size, represented by bin numbers with a bin width of 10. Bin #10, e.g., contains all sizes from 90 to 99. Bin #1000 contains the sizes 9990 to 9999 and, additionally, all other ones larger than 9999. The data were taken over a period of  $2 \cdot 10^7$  time steps. Note the appearance of the first peak around bin #20 which is explained in the text. The left hand side of the figure represents behavior according to a randomized devil's staircase function.

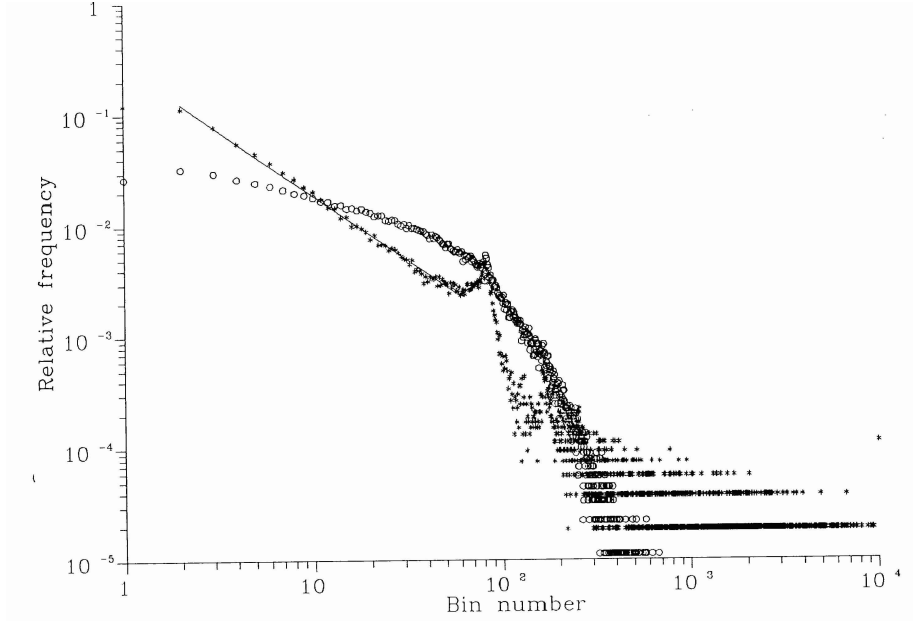


Figure 7: Same as in Figure 6, but for a larger memory  $t_{mem} = 800$  and for a larger number of bins to make the occurrence of very large time plateaus more clear. The first peak now shows up at around bin #80. The circled data represent the originally introduced noise-free model of fractal evolution [9, 10] indicating a sharp cutoff of the plateau sizes. The fit indicates the slope due to a randomized devil's staircase function.

sizes of order  $O(400)$ ) represent a direct effect of the chosen size of the system's memory  $t_{mem} = 200$ . Succeeding boosts occurring with temporal distances of order  $O(k \cdot t_{mem})$ ,  $k = 1, 2, \dots$  are causally related due to the evolution rule (3) and the values of the systems variables. The remaining boost distances are clearly not directly related and their distribution represents a genuine emergent property of the systems dynamics.

As long as we use a systems memory, this perturbation of causally unrelated boost distances by causally related ones seems to be inevitable, but the moment of the peak's first occurrence can be shifted towards larger plateau sizes as shown in Figure 7. In that case, a memory depth of  $t_{mem} = 800$  was chosen. Accordingly, the peak shows up at about bin #80. Up to this value, the frequency  $f(s)$  of plateau sizes  $s$  scales according to

$$f(s) \propto s^{-1.17 \pm 0.01} \quad (6)$$

thus indicating a randomized devil's staircase function [16, 6]. The exponent obtained above represents a robust property of the system in spite of its inherent contingency indicated by Figure 5. For comparison, the circled data in Figure 7

represent the distribution of boost distances due to our evolution rules used earlier [9, 10], where no noise threshold condition had been incorporated. The observed fragments' distribution all over the spatiotemporal plane in the noise-free model is reflected in the sharp cutoff of frequencies for plateau sizes beyond  $s \approx 10^4$ .

## 2.2 Self-organized evolution of fractal evolution

As has already been remarked in the previous section, fractal evolution in the true sense of the word is effectively realized only if the interval width  $\epsilon$  is allowed to acquire different values during the systems evolution. According to a recently introduced idea [11, 12], to be further elaborated here, we impose an additional long-term control cycle leading to an adaptive change of  $\epsilon$  on the next higher level of the system's hierarchical nesting of feedback loops.

We thus let the system be driven by fluctuations of  $\tilde{\tau}_{exp}$  measured with the same  $\epsilon$  during two succeeding long time spans or generations ( $n, n+1$ ). The difference  $\tilde{\tau}_{exp}(n+1) - \tilde{\tau}_{exp}(n)$  is practically always nonzero due to the finite time interval of data taking. To implement an adaptive change of  $\epsilon$  or resolution  $1/\epsilon$ , respectively, with regard to an ever changing ruggedness of the whole fitness landscape, this difference is fed back into the consecutive value of  $\epsilon$  via the difference quotient of the power-law (5)

$$\frac{\Delta\tilde{\tau}}{\tilde{\tau}} = b \frac{\Delta\epsilon}{\epsilon} , \quad (7)$$

leading to

$$\Delta\epsilon = \epsilon_{n+1} - \epsilon_n = \frac{\epsilon_n}{b} \cdot \frac{\tilde{\tau}_{n+1} - \tilde{\tau}_n}{\tilde{\tau}_n} . \quad (8)$$

Since the last term of Eq. (8) is generally non-zero due to the fluctuations of the mean lifetime, a different relative interval width results governing the two succeeding generations, and is determined by

$$\epsilon_{n+2} := \epsilon_{n+1} = \epsilon_n \left( 1 + \frac{1}{b} \cdot \frac{\tilde{\tau}_{n+1} - \tilde{\tau}_n}{\tilde{\tau}_n} \right) . \quad (9)$$

The geometrical analogy to the analytical determination of the next value of  $\epsilon_{n+2}$  or  $\epsilon_{n+1}$ , respectively, is given as follows: the latter lies at the intersection of the tangent at  $(\epsilon_n, \tilde{\tau}_n)$  belonging to the theoretical curve  $\tilde{\tau}_n = a' \cdot \epsilon_n^b$  on one hand, and the horizontal line through  $\tilde{\tau}_{n+1}$  on the other.

As a main result, we obtain a progressive alteration of  $\epsilon$  or the resolution  $1/\epsilon$ , respectively, within the system's evolution which we denote as "hierarchically emergent fractal evolution" (HEFE). In effect, HEFE constitutes a fluctuation driven and adaptive mechanism for the gradual increase of the mean lifetimes of the emerging patterns, i.e. for the expansions of regions of high fitness in the fitness landscape.

In Figure 8, three examples of temporal evolutions of the mean lifetime per generation are shown according to three different time spans of each generation

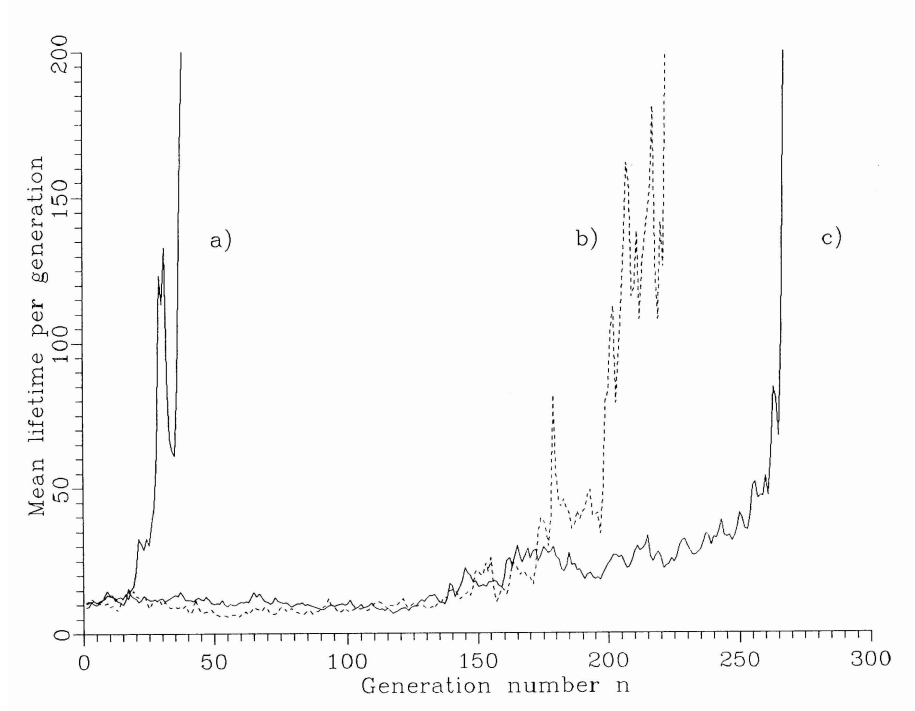


Figure 8: Hierarchically emergent fractal evolution (HEFE) for three different values of time spans of data taking with particular  $\epsilon$  ("generations"). The time span for each generation is given by 2000 time steps for curve a), 5000 for curve b), and 10000 for curve c). The starting value of  $\epsilon$  for all curves is  $\epsilon_0 = 10\%$ . Apart from the obvious time asymmetry of the evolution, note also the characteristic stepwise increases as well as decreases of the mean lifetimes per generation, thus indicating two opposing trends in the short-term dynamics. In the long run, however, the mean lifetime is bound to increase.



during which the mean lifetime is determined. Although fluctuations are allowed with equal opportunity for decreasing and increasing lifetimes, respectively, a long-term increase of the mean lifetimes is observed practically in all cases and has its origin in the functional property of the power-law (5): Denoting the deviation of the mean lifetime by  $\tilde{\tau}_{n+1} - \tilde{\tau}_n =: \eta^\pm \cdot \tilde{\tau}_n$ , and assuming one positive-valued deviation  $\eta^+$  for the consecutive generations  $(n, n+1)$  and a negative-valued one  $\eta^-$  of about equal size  $\eta^+ \approx -\eta^-$  for the succeeding ones  $(n+2, n+3)$ , one obtains altogether a clear tendency towards decreasing relative interval widths

$$\epsilon_{n+4} \approx \epsilon_n (1 - |\frac{\eta^\pm}{b}|^2) < \epsilon_n , \quad (10)$$

leading to an average increase of the mean lifetime  $\tilde{\tau}$  per generation. If  $\tilde{\tau}$  would depend, e.g., exponentially on  $\epsilon$ , like  $\tilde{\tau} \propto e^{-\epsilon}$ ,  $\epsilon$  would only oscillate between two fixed values.

For relatively small time spans, i.e. for curve a) with 2000 time steps per generation, the fluctuation of the lifetimes is larger, of course, than for 10000 time steps. Therefore, the observed drastic increase of the mean lifetimes will occur sooner. In sum, the systems dynamics makes possible a long-term growth of each species' lifetime and thus also of its complexity: larger lifetimes of high fitness periods increase, e.g. via "learning", both the cognitive performances as well as the probability for survival of the species and, consequently, also the probability for genetic improvement via mutational mechanisms. As far as the cognitive functions are concerned, their improvement increases the lifetimes of high fitness values, and so on. We reach the limits of our model when the mean lifetimes in Figure 8 reach the size of the system's memory  $t_{mem}$ , because then fractal evolution gets disturbed [10] and new boundary conditions would have to be considered that might constrain the further evolution effectively.

Finally, we briefly discuss the evolution of the system's entropy, which measures the fitness of the whole ensemble of species, and is simply chosen as the relative Shannon information entropy [10]

$$\frac{S}{S_{max}} = \frac{-1}{\ln N} \sum_{j=1}^N \rho(t, j) \cdot \ln \rho(t, j) . \quad (11)$$

We can allocate the various activities within the systems evolution with regard to their specific entropy behavior in the following way. A site's enhancement, i.e., an increased single species' fitness value, lowers the system's entropy at that time step due to the enlargement of the values' differences within the array. The effect of the noise threshold and the decay of the fragments due to Eq. (1) are entropy increasing processes. Since the systems evolution with a given fixed value of  $\epsilon$  yields a stationary pattern production characterized by the fractal evolution exponent, an average value of the above described entropy contributions summed up for an appropriate long time interval is obtained for that specific  $\epsilon$ . The larger the value of  $\epsilon$ , the shorter the mean lifetime of the fragments and, consequently, the more rugged the fitness landscape will appear, thereby lowering the normalized entropy per time interval (cf. Figure 9).

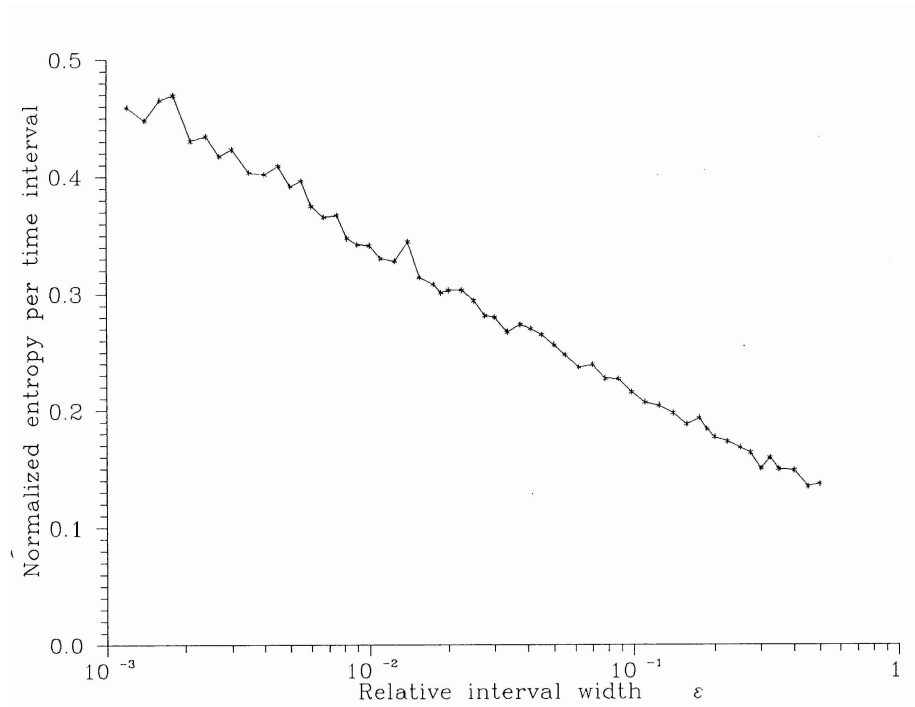


Figure 9: Normalized entropy per 10000 time steps versus the relative interval width in a semi-logarithmic plot. Since the long-term behavior of HEFE develops towards larger mean lifetimes  $\bar{\tau}$ , and, therefore, towards smaller values of  $\epsilon$ , the entropy of the evolving system increases on the average.

With respect to the HEFE-mechanism, this means that the total entropy per time interval increases on the average due to the growth of the mean lifetimes. That is, within the scenario of macroevolution this effect can be considered as tendency towards maximal fitness of the whole ensemble of species under constant boundary conditions. Thus, *internal* evolutions within a species towards higher complexity are accompanied by a complementary, *external* increase of the entropy of the fitness landscape.

### 3 Conclusions

The scaling behavior of certain observables in dynamical systems is of particular relevance in a wide range of systems, be they geophysical, economical or biological, for example. Within the theoretical framework of the SOC theory some features of macroevolution have recently also become testable via a kind of “experimental paleontology” [15]. They are made plausible by the concept of a system’s critical state which is reached after a certain evolutionary time,

and which thereby exhibits a power-law behavior of the frequency of mutation activities with regard to their sizes. Yet they suffer from being trapped within the steady-state property of the system’s dynamics.

In this paper we have proposed a model for macroevolution based on concepts differing from the SOC model. Apart from some basic qualitative similarities (cf. Figs. 4 and 5), we obtain substantially different results, primarily with regard to the time-invariant behavior of the system’s emerging order parameter: the power-law obtained in our model reflects a universal feature named “fractal evolution”, which can be based on a variety of underlying mechanisms, including the option of a memory-based feedback operation. The four major problems specified in the introduction in order to overcome some weak points in existing models of macroevolution are solved by the implementation of a second feedback operation. The latter transforms the mere functional property of “fractal evolution” of the system’s fitness landscape via a fluctuation-based iterative mechanism into the dynamical process called “hierarchically emergent fractal evolution” (HEFE). In this way, a self-organized potential growth emerges on a long-term scale, such that the internal complexity of each species may gradually increase. However, throughout this work we have deliberately avoided a narrow definition of the term “complexity”, or a choice among the proliferating definitions in the literature, respectively [5]. Instead, we have merely considered beneficial fitness domains for each species in the sense of potentials to evolve towards higher complexity, irrespective of the underlying concrete (self-organized) mechanisms. One main result of our study is that in our model such potentials grow with elapsing time.

We also emphasize the important role of randomness in our model, which is effective on various hierarchical levels. At the basic level of pattern generation, we observe a strong sensitivity of the patterns’ signature to slight variations of the initial conditions, similar to the features of deterministic chaos. An emerging global measure, irrespective of local system fluctuations, has been obtained in the form of the fractal evolution exponent. The incorporation of a noise threshold constraining the range of operational fitness values for each species enables the systems’ patterns to walk randomly across the whole array (cf. Figs. 2 and 4), thereby producing activity/mutation patterns obeying a randomized devil’s staircase function. As in the SOC model [2, 6], small deviations in the order of mutation events produce significant deviations from the course of the accumulated activity pattern (cf. Figure 5). The globally invariant measure in this case is given by the slope of the distribution function for the frequency of the periods of stasis versus their sizes (cf. Figs. 6 and 7). Moreover, at the level of the self-organized change of the resolution-like parameter  $\epsilon$ , the natural fluctuation of the order parameter  $\tilde{\tau}$  within two runs (“generations”) under the same conditions iteratively serves as driving force towards a changing  $\epsilon$ . The direction of this change appears on small time scales as a random walk. However, the long-time tendency towards the irreversible decrease of  $\epsilon$ , and thus towards the increase of the mean lifetimes of the high fitness domains for each species, respectively, is firmly anchored in the HEFE mechanism (cf. Figure 8). More generally speaking, it is rooted in the basic

mathematical properties of the power-law describing fractal evolution, and it leads in the long run to a mutual positive enhancement of potential cognitive abilities for all species on one hand, and lifetimes with high fitness values on the other.

Finally, the potential development of individual species towards gradually higher complexity (as represented by an evolution towards ever lower values of  $\epsilon$ ) is accompanied by a tendency towards highest entropy values for the whole fitness landscape under constant boundary conditions (cf. Figure 9). The HEFE mechanism can thus be interpreted such that a single species is constantly engaged, via the possibilities of beneficial selection versus detrimental extinction, in a struggle for higher fitness values, whereas there exists a global tendency of ever higher fitness values to emerge for the whole ensemble of species.

## References

- [1] Ausloos M. and Vandewalle N., Algorithmic models for evolution, *Europhys. News* **26** (1995) pp. 55-56
- [2] Bak P. and Paczuski M., Complexity, contingency, and criticality, *Proc. Natl. Acad. Sci.* **92** (1995) pp. 6689-6696
- [3] Bak P. and Sneppen K., Punctuated equilibrium and criticality in a simple model of evolution, *Phys. Rev. Lett.* **71** (1993) pp. 4083-4086
- [4] Bak P., Tang C. and Wiesenfeld K., Self-organized criticality: an explanation of  $1/f$  noise, *Phys. Rev. Lett.* **59** (1987) pp. 381-384, Self-organized criticality, *Phys. Rev.* **A38** (1988) pp. 364-374.
- [5] See, e.g., Bates J.E. and Shepard H.K., Measuring complexity using information fluctuation, *Phys. Lett.* **A172** (1994) pp. 416-425.
- [6] Boettcher S. and Paczuski M., Exact results for spatiotemporal correlations in a self-organized critical model of punctuated equilibrium, *Phys. Rev. Lett.* **76** (1996) pp. 348-351
- [7] Eldredge N. and Gould S. J., in *Models in Paleobiology*, ed. by T.J.M. Schopf T. J. M., (Freeman, San Francisco, 1972)
- [8] Elena S.E., Cooper V.S. and Lenski R.E., Punctuated evolution caused by selection of rare beneficial mutations, *Science* **272** (1996) pp. 1802-1804 and p. 1741
- [9] Fussy S. and Grössing G., Fractal evolution of normalized feedback systems on a lattice, *Phys. Lett.* **A186** (1994) pp. 145-151
- [10] Fussy S., Grössing G. and Schwabl H., Fractal evolution in deterministic and random models, *Int. J. Bifurcation and Chaos* **6**(11) (1996) pp. 1977-1995

- [11] Fussy S., Grössing G. and Schwabl H., Fractal evolution in discretized systems. In *Self-Organization of Complex Structures: From Individual to Collective Dynamics*, ed. by Schweitzer F. (Gordon and Breach, London, 1996) in press
- [12] Fussy S., Grössing G. and Schwabl H., Hierarchically emergent fractal evolution. In *Cybernetics & Systems '96 Vol. I*, ed. by Trappl R. (Vienna, 1996) pp.189-194
- [13] Gould S. J. and Eldredge N., Punctuated equilibrium comes of age, *Nature* (1993) **366** pp. 223-227
- [14] Kauffman S. A., *The origins of Order* (Oxford Univ. Press, New York Oxford, 1993)
- [15] Lenski R. E. and Triviso M., Dynamics of adaptation and diversification: A 10,000-generation experiment with bacterial populations, *Proc. Natl. Acad. Sci.* **91** (1994) pp. 6808-6814
- [16] Mandelbrot B. B., *The fractal geometry of nature* (W. H. Freeman, San Francisco, 1982) pp.286-287
- [17] Schuster P., Molekulare Evolution an der Schwelle zwischen Chemie und Biologie. In *Die Evolution der Evolutionstheorie*, ed. by Wieser W. (Spektrum Akademie Verlag, Heidelberg-Berlin-Oxford, 1994) pp.49-76
- [18] Sneppen K., Bak P., Flyvbjerg H. and Jensen M.H., Evolution as a self-organized critical phenomenon, *Proc. Natl. Acad. Sci.* **92** (1995) pp. 5209-5213
- [19] Solé R. V. and Manrubia S. C., Extinction and self-organized criticality in a model of large-scale evolution, *Phys. Rev.* **E54** (1996) pp. R42-R45
- [20] Vandewalle N. and Ausloos M., Self-organized criticality in phylogenetic-like tree growths, *J. Phys. I France* **5** (1995) pp. 1011-1025